

Large-Scale Structure Formation in the Quasi-linear Regime

F. Bernardeau

*Service de Physique Théorique, C.E. de Saclay,
F-91191 Gif-sur-Yvette, France*

Abstract

The understanding of the large-scale structure formation requires the resolution of coupled nonlinear equations describing the cosmic density and velocity fields. This is a complicated problem that, for the last decade, has been essentially addressed with N-body simulations. There is however a regime, the so-called quasi-linear regime, for which the relative density fluctuations are on average below unity. It is then possible to apply Perturbation Theory techniques where the perturbation expansions are made with respect to the initial fluctuations. I review here the major results that have been obtained in this regime.

1 The Gravitational Instability Scenarios

Perturbation Theory (PT) has had important developments in the last few years simultaneously from theoretical, numerical and observational points of view. These techniques allow indeed to explore nonlinear features revealed in the statistical properties of the large-scale structures of the Universe, for which precise and robust data are now available. The general frame of these calculations is based on the dynamics of a self-gravitating *pressure-less* fluid. The large-scale structures are then assumed to have gravitationally grown from small initial fluctuations. It is important to note that in the following these initial fluctuations will be assumed to follow a Gaussian statistics. That excludes a priori exotic models that make intervene topological defects as seeds of structure formation.

By linearizing the field equations, i.e. when the quadratic coupling between the fields is neglected, one can compute the growth rate of the fluctuations. This allows to compare for instance the Cosmic Microwave Background temperature anisotropies as measured by the COBE satellite with the local density fluctuations observed in galaxy catalogues. The linear approximation cannot be used however to explore the statistical properties of the density field: the local fluctuations are just amplified, their shapes are not changed, and therefore the linear density field remains Gaussian if it obeyed such statistics initially.

2 The Perturbation Theory

The principles of these calculations have been initially presented by Peebles [35], then explored in more details in a series of recent papers [18, 22, 12, 3, 27, 28, 33, 5, 37, 38]. The starting point of all these calculations is the system of field equations, Continuity, Euler and Poisson equations, describing a single stream pressure-less fluid.

The density and velocity fields which satisfy those equations are then expanded with respect to the initial fluctuation field,

$$\delta(t, \mathbf{x}) = \sum_i \delta^{(i)}(t, \mathbf{x}), \quad \mathbf{u}(t, \mathbf{x}) = \sum_i \mathbf{u}^{(i)}(t, \mathbf{x}). \quad (1)$$

The fields $\delta^{(1)}(t, \mathbf{x})$ and $\mathbf{u}^{(1)}(t, \mathbf{x})$ are just the local linearized density and velocity fields. They are linear in the initial density field. The higher order terms, $\delta^{(2)}$, $\delta^{(3)}$,... are respectively quadratic, cubic,... in the initial density field, and, therefore, do not obey a Gaussian statistics.

2.1 The Density Field

The time and space dependences of the linearized density field, $\delta^{(1)}$, factorize so that it can be written,

$$\delta^{(1)}(t, \mathbf{x}) = D(t) \int d^3 \mathbf{k} \delta(\mathbf{k}) \exp(i\mathbf{k}\mathbf{x}), \quad (2)$$

where $\delta(\mathbf{k})$ are the Fourier transforms of the initial density field. They are assumed to form a set of Gaussian variables. Their statistical properties are then entirely determined by the shape of the power spectrum, $P(k)$, defined by,

$$\langle \delta(\mathbf{k}) \delta(\mathbf{k}') \rangle = \delta_{\text{Dirac}}(\mathbf{k} + \mathbf{k}') P(k), \quad (3)$$

where $\langle \cdot \rangle$ denotes ensemble averages over the initial conditions. The function $D(t)$ is determined by the cosmological parameters. It is proportional to the expansion factor $a(t)$ for an Einstein-de Sitter universe. In general it has been found to depend on the cosmological density Ω in such a way that $(d \log D / d \log a) \approx \Omega^{0.6}$ [35] and to be very weakly dependent on the cosmological constant Λ [29].

The higher order terms can all be recursively obtained from the linear term. In general one can write the i^{th} order term as [22],

$$\delta^{(i)}(t, \mathbf{x}) = D^i(t) \int d^3 \mathbf{k}_1 \dots d^3 \mathbf{k}_i \delta(\mathbf{k}_1) \dots \delta(\mathbf{k}_i) \exp[i\mathbf{x} \cdot (\mathbf{k}_1 + \dots + \mathbf{k}_i)] F(\mathbf{k}_1, \dots, \mathbf{k}_i), \quad (4)$$

where $F(\mathbf{k}_1, \dots, \mathbf{k}_i)$ is a homogeneous function of the angles between the different wave vectors. Note that the time dependence given here is only approximate for a non Einstein-de Sitter Universe. It is however a very good approximation [3, 12, 4, 5].

2.2 The Velocity Field

For the velocity field the situation is very similar. We have first to notice that in the single flow approximation the vorticity is expected to be diluted by the expansion (eg. [35]) and thus to be negligible *at any order* of the perturbation expansion. Then it is more natural to present the properties of the velocity field in terms of the local divergence (expressed in units of the Hubble constant),

$$\theta(t, \mathbf{x}) \equiv \frac{\nabla_{\mathbf{x}} \cdot \mathbf{u}(t, \mathbf{x})}{H(t)}. \quad (5)$$

We then have,

$$\theta^{(1)}(t, \mathbf{x}) = \frac{d \log D}{d \log a} \delta^{(1)}(t, \mathbf{x}) \approx \Omega^{0.6}(t) \delta^{(1)}(t, \mathbf{x}). \quad (6)$$

The higher order terms can be written

$$\theta^{(i)}(t, \mathbf{x}) \approx \Omega^{0.6}(t) D^i(t) \int d^3 \mathbf{k}_1 \dots d^3 \mathbf{k}_i \delta(\mathbf{k}_1) \dots \delta(\mathbf{k}_i) \exp[i\mathbf{x} \cdot (\mathbf{k}_1 + \dots + \mathbf{k}_i)] G(\mathbf{k}_1, \dots, \mathbf{k}_i), \quad (7)$$

where G is another homogeneous function, different from F . Note that in general the time dependence of $\theta^{(i)}$ is not the power i of the time dependence of $\theta^{(1)}$. We will see that it induces remarkable statistical properties for the local velocity field.

2.3 Implications for the Statistical Properties of the Cosmic Fields

In general the consequences of the existence of higher order terms can be separated in two categories: these terms affect the mean growth rate of the fluctuations and introduce new statistical properties because of their non-Gaussian nature. I will briefly review both aspects here.

3 The Mean Growth Rate of the Fluctuations

The mean growth rate of the fluctuation can be calculated from the shape and magnitude of the variance of the local density contrast [26, 32, 38], or equivalently of the evolved power spectrum [33, 25]. For instance the variance, $\langle \delta^2 \rangle$, can be calculated using the expansion in (1),

$$\langle \delta^2 \rangle = \langle (\delta^{(1)} + \delta^{(2)} + \dots)^2 \rangle. \quad (8)$$

By re-expanding this expression with respect to the initial density field one gets,

$$\langle \delta^2 \rangle = \langle (\delta^{(1)})^2 \rangle + 2 \langle \delta^{(1)} \delta^{(2)} \rangle + \langle (\delta^{(2)})^2 \rangle + 2 \langle (\delta^{(1)} \delta^{(3)})^2 \rangle + \dots \quad (9)$$

The term $\langle \delta^{(1)} \delta^{(2)} \rangle$ is zero because it is cubic in the initial Gaussian variables. The calculation of the corrective terms (the so-called “loop corrections”, see [22, 3, 37, 38]), $\langle (\delta^{(2)})^2 \rangle + 2 \langle \delta^{(1)} \delta^{(3)} \rangle$, can be done from the recursive solution of the field equations. In practice these calculations become rapidly very complicated but they can be simplified in case of a power law spectrum,

$$P(k) \propto k^n. \quad (10)$$

Thus for $n = -2$ one gets

$$\langle \delta^2 \rangle = \langle \delta_{\text{lin}}^2 \rangle + \frac{1375}{1568} \langle \delta_{\text{lin}}^2 \rangle^2 \approx \langle \delta_{\text{lin}}^2 \rangle + 0.88 \langle \delta_{\text{lin}}^2 \rangle^2 \quad (11)$$

where δ_{lin} is the linearized density contrast, $\delta_{\text{lin}} = \delta^{(1)}$. This prediction can be compared with numerical results obtained from N -body codes. An interesting way to compare the two is to use the phenomenological description of the nonlinear growth rate of the fluctuations proposed by Hamilton et al. [23]. This description relates the mean linear density contrast at the scale R_{lin} to the full non-linear one at the scale $R_{\text{non-lin}}$ defined by

$$R_{\text{non-lin}}^3 (1 + \langle \delta^2 \rangle) = R_{\text{lin}}^3. \quad (12)$$

The universal transform proposed by Hamilton et al. (given here in terms of the power spectrum) is presented in Fig. 1 (solid line) and compared to the prediction (11), (short dashed line). The latter gives remarkably well the position of the departure from the pure linear regime (straight line). On the other hand the position of this transition is quite poorly given by the Zel’dovich approximation (long dashed line).

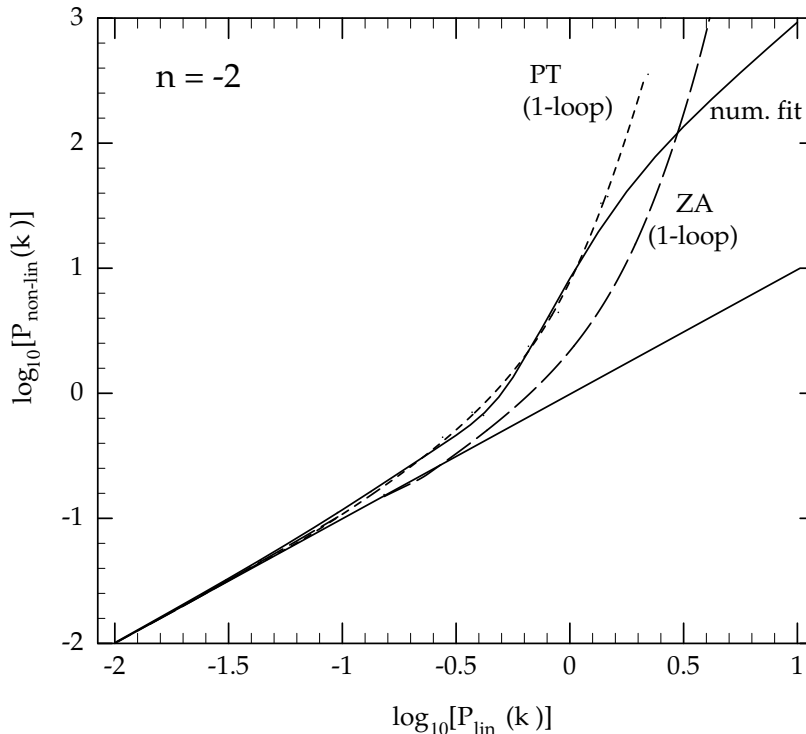


Figure 1. Comparison of the PT predictions (11) with the Hamilton et al. [23] prescription for the growth rate of the fluctuation (solid line) in case of $P(k) \propto k^{-2}$. The short dashed line is the prediction of the next-to-leading order Perturbation Theory result [38], and the straight line is the linear theory prediction (figure taken from [38]).

Surprisingly the corrective terms are finite only for $n < -1$. For n larger than -1 the loop terms contain a divergence so that the result explicitly depends on a cutoff k_c introduced in the shape of the power spectrum at large k . Thus when $(R k_c)$ is large we have,

$$\langle \delta^2 \rangle = \langle \delta_{\text{lin}}^2 \rangle + C_n (k_c R)^{n+1} \langle \delta_{\text{lin}}^2 \rangle^2 \quad (13)$$

where R is the filtering radius. The existence of this divergence was not really expected since the numerical results do not indicate any significant change of behavior for $n \approx -1$. One could argue that in practice this is not a relevant problem since in realistic scenarios (like the CDM power spectrum) the index reaches $n = -3$ at small scale, so that the corrective terms are naturally regularized. However with such an interpretation it implies that the growth of the very large scale fluctuations is fed with smaller scale fluctuations, which would be slightly surprising in view of the numerical results accumulated over the last few years. Another possible explanation is that the higher order corrections induce other divergences that cancel each other (a phenomenon quite common in statistical physics). Then the corrective terms to the linear growth rate would not be proportional to the square of $\langle \delta_{\text{lin}}^2 \rangle$ but to a smaller power of it. Future analytic investigations may be able to throw light on this problem.

4 The Emergence of non-Gaussian Features

4.1 The Moments

The other major consequence of the existence of non-linear terms in (1) is the apparition of non-Gaussian properties. Although it is possible to characterize non-Gaussian features in many different ways, most of the efforts have been devoted to properties of the one-point probability distribution

function (PDF) of the local density. More particularly, attention has been focussed on the moments of this distribution and how they are sensitive to non-linear corrections. In his treatise [35], Peebles already considered the implications of second order perturbation theory for the behavior of the third moment of the local density in case of initial Gaussian fluctuations. Indeed, using the expansion (1), the third moment reads,

$$\langle \delta^3 \rangle = \langle (\delta^{(1)} + \delta^{(2)} + \dots)^3 \rangle = \langle (\delta^{(1)})^3 \rangle + 3 \langle (\delta^{(1)})^2 \delta^{(2)} \rangle + \dots, \quad (14)$$

and what should be the dominant term of this series, $\langle (\delta^{(1)})^3 \rangle$, is identically zero in case of Gaussian initial conditions. As a consequence the third moment is actually given by

$$\langle \delta^3 \rangle \approx 3 \langle (\delta^{(1)})^2 \delta^{(2)} \rangle. \quad (15)$$

Peebles calculated this expression neglecting the effects of smoothing and found (for an Einstein-de Sitter Universe),

$$\langle \delta^3 \rangle \approx \frac{34}{7} \langle \delta_{\text{lin}}^2 \rangle^2, \quad (16)$$

so that the ratio, $\langle \delta^3 \rangle / \langle \delta^2 \rangle^2$, is expected to be finite at large scale. It is actually possible to extend this quantitative behavior to higher order moment and to show that the cumulants (i.e., the connected parts of the moments) are related to the second moment so that the ratios,

$$S_p = \langle \delta^p \rangle_c / \langle \delta^2 \rangle^{p-1}, \quad (17)$$

are all finite at large scale. As mentioned before, the coefficient S_3 was computed by Peebles [35], Fry [18] derived S_4 and eventually Bernardeau [3] gave the whole series of these coefficients.

Unfortunately these early calculations did not take into account the filtering effects, that is that the ensemble averages should be done on the local smoothed fields. This problem was addressed numerically by Goroff et al. [22] for a Gaussian window function for the third and fourth moments. More recently these two coefficients have been calculated analytically and semi-analytically in [28, 31] for this window function. However, the results turn out to be simpler in case of a top-hat window, as it was noticed by Juszkiewicz et al. [27] for S_3 and power law spectra. The coefficients S_3 and S_4 were calculated for this window in [4] for any spectrum and any cosmological models. Eventually Bernardeau [5] proposed a method to derive the whole series of these coefficients from the spherical collapse dynamics.

I recall here the expression of the first two coefficients S_3 and S_4 , as a function of the shape of the second moment,

$$S_3(R) = \frac{34}{7} + \gamma(R); \quad (18)$$

$$S_4(R) = \frac{60712}{1323} + \frac{62\gamma(R)}{3} + \frac{7\gamma(R)^2}{3} + \frac{2}{3} \frac{d\gamma(R)}{d \log R}; \quad (19)$$

with

$$\gamma = \frac{d \log \sigma^2(R)}{d \log R}. \quad (20)$$

One can notice that S_3 depends only on the local slope, and that S_4 also depends (but weakly) on the variations of that slope. These results are valid for an Einstein-de Sitter Universe but are found to be weakly Ω and Λ dependent [12, 3, 4].

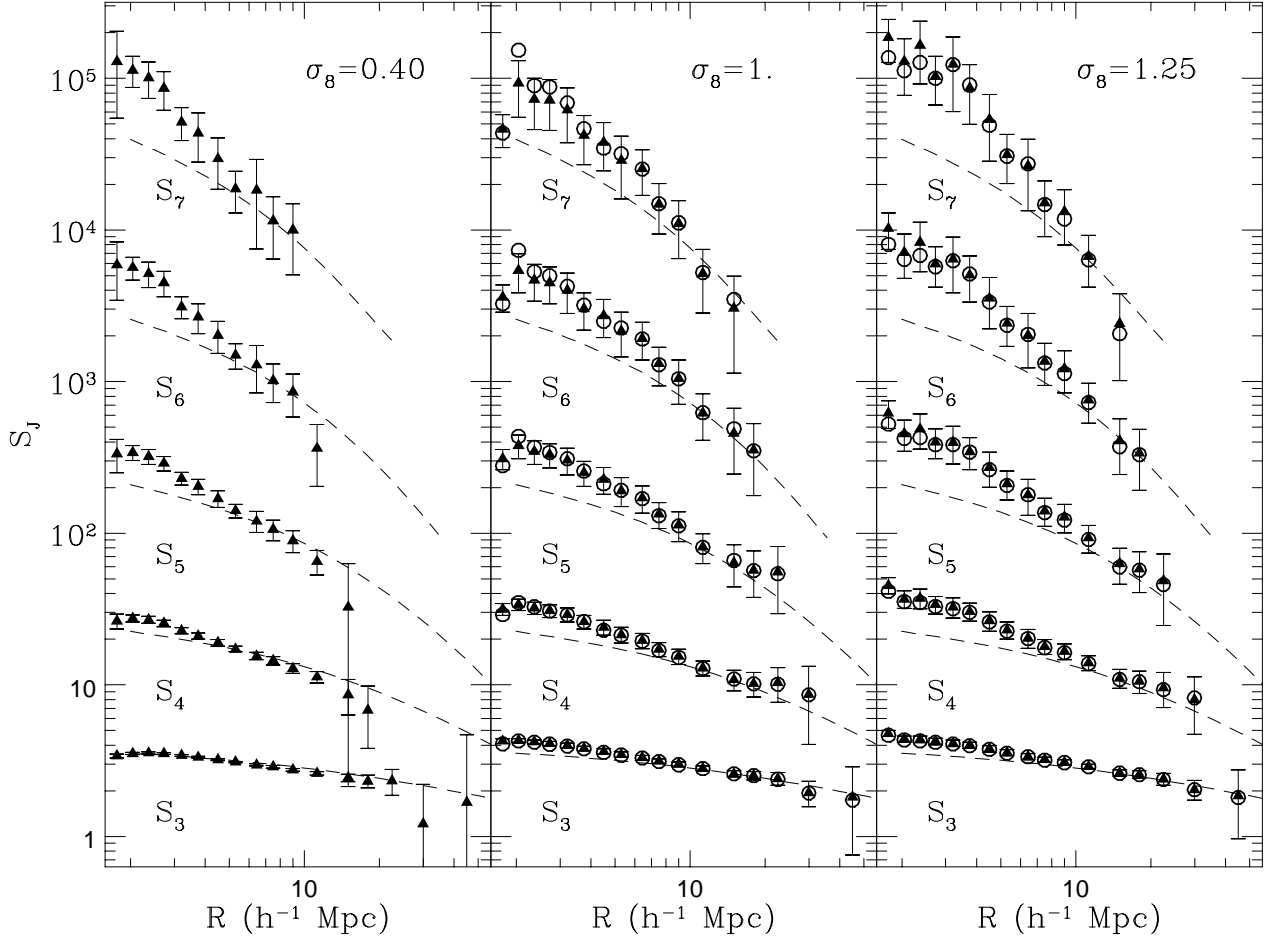


Figure 2. Comparison of PT predictions with results of numerical simulations with CDM initial conditions for moments of the local density contrast. The PT results (dashed lines) are compared to the measured S_p coefficients as a function of radius for three different time-steps (figure taken from [2]).

These coefficients have been tested against numerical results by different groups [12, 4, 2, 31] and have been found to be in extremely good agreement with the numerical results. In particular as shown in Fig.2, it has been found that the measured S_p coefficients are in good agreement with the PT results up to $p = 7$ as long as the variance $\langle \delta^2 \rangle^{1/2}$ is lower than unity [2]. This constraint does not seem to become tighter for higher orders.

4.2 From Cumulants to PDF-s

The shape of the PDF and the values of the cumulants are obviously related. When a limited number of cumulants is known it is possible to reconstruct some aspect of the shape of the PDF using the so-called Edgeworth expansion (see [28, 7]). But actually as the whole series of the cumulants is known for top-hat filtering it is possible to invert the problem (at least numerically) and build the PDF from the generating function of the cumulants (see [1] for the general method and [3, 5] for the application to PT results). This method is justified by the fact that the S_p coefficients converge to their asymptotic PT values at roughly the same rate, i.e. for the same values of $\langle \delta^2 \rangle$ (Fig. 2).

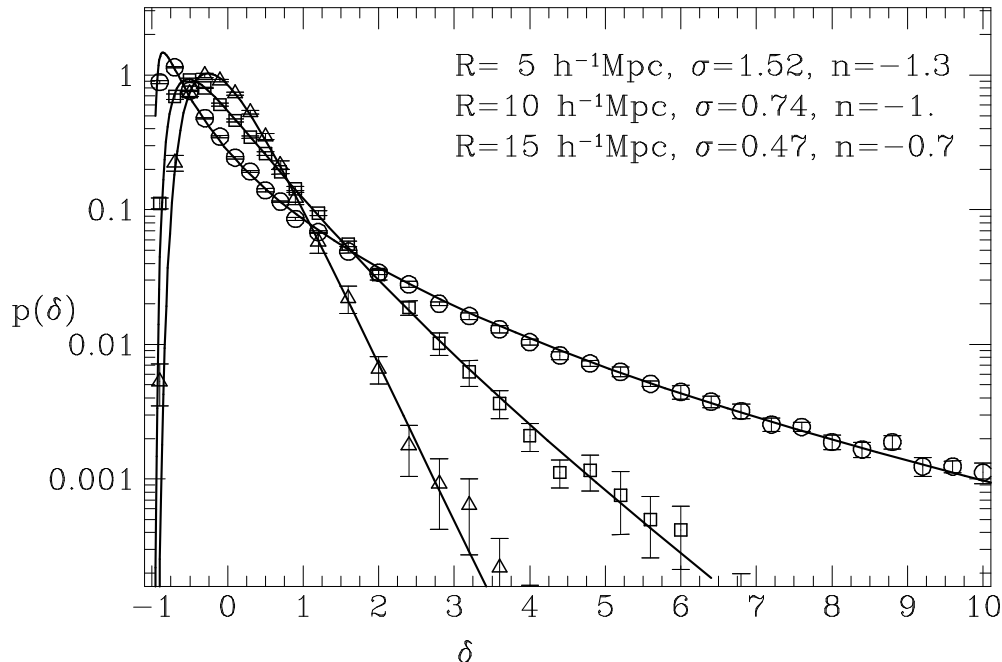


Figure 3. Comparison of PT predictions with results of numerical simulations with CDM initial conditions for the shape of the one-point PDF of the density contrast. The density PDF has been measured at three different radius, $R = 5 \text{ h}^{-1}\text{Mpc}$ (circles), $R = 10 \text{ h}^{-1}\text{Mpc}$ (squares), $R = 15 \text{ h}^{-1}\text{Mpc}$ (triangles) and compared to the PT predictions calculated from the measured values of the variance and the local index (figure taken from [5]).

In Fig. 3, I present a comparison of the PT results obtained in such a way to the numerical measurements of PDF-s. Three different smoothing radii have been chosen. For each radius one can get the value of the initial index, and the value of the variance. The predicted PDF-s are entirely determined by those two numbers. As it can be seen the agreement is extremely good.

5 Comparison with data

These successes have given confidence in the validity of the PT results and have boosted investigations in the available galaxy catalogues. Using the IRAS galaxy catalogue Bouchet et al. [13] measured the 3rd and 4th moment of the one-point PDF of the local galaxy density. The observed relation between the third moment and the second is the following,

$$\langle \delta_{\text{IRAS}}^3 \rangle \approx 1.5 \langle \delta_{\text{IRAS}}^2 \rangle^2. \quad (21)$$

It is a strong indication in favor of Gaussian initial conditions since the exponent is indeed the one expected from PT. The coefficient however is lower from what is expected, but the comparison with quantitative predictions is complicated for two reasons. The galaxy positions are known only in redshift space (that is that their distance is assumed to be proportional to their line-of-sight velocity), and IRAS galaxies might be strongly biased with respect to the mass distribution. The first problem has been addressed in [24] where it is shown with adapted PT calculations that the effects of redshift space distortion on S_3 are small at large scale. It has been also investigated numerically in [30]. The fact that the measured coefficient, 1.5, is smaller than what is expected (by a factor of about 1.7) is then probably due to biases in the galaxy distribution. In case of the IRAS galaxies this is not too surprising since those galaxies are known to be under-populated (compared to bright galaxies) in very dense areas.

For these reasons a lot of interest has been devoted recently to the APM angular galaxy catalogue. The fact that it has more than 1,300,000 objects makes it the largest galaxy catalogue now available and a perfect domain of investigation. Measurements of the S_p coefficients have been made by Gaztañaga [19] for $p \leq 7$. Comparison with PT predictions are however not straightforward because of the projection effects with which the relations (18,19) for S_3 and S_4 are not valid anymore.

Adapted calculations that take into account this new geometry and using the small angle approximation have been made in [6] for any order of cumulants but assuming a power law spectrum. These results have been recently extended in [36] for any shape of power spectrum. In fig 4. I present the comparison of the measured S_3 and S_4 coefficients as a function of the smoothing angle (triangles) compared to the predicted ones from PT (solid lines). The latter have been calculated with either the small angle approximation or with a direct Monte-Carlo integration for which no such approximation is required (for S_3 only).

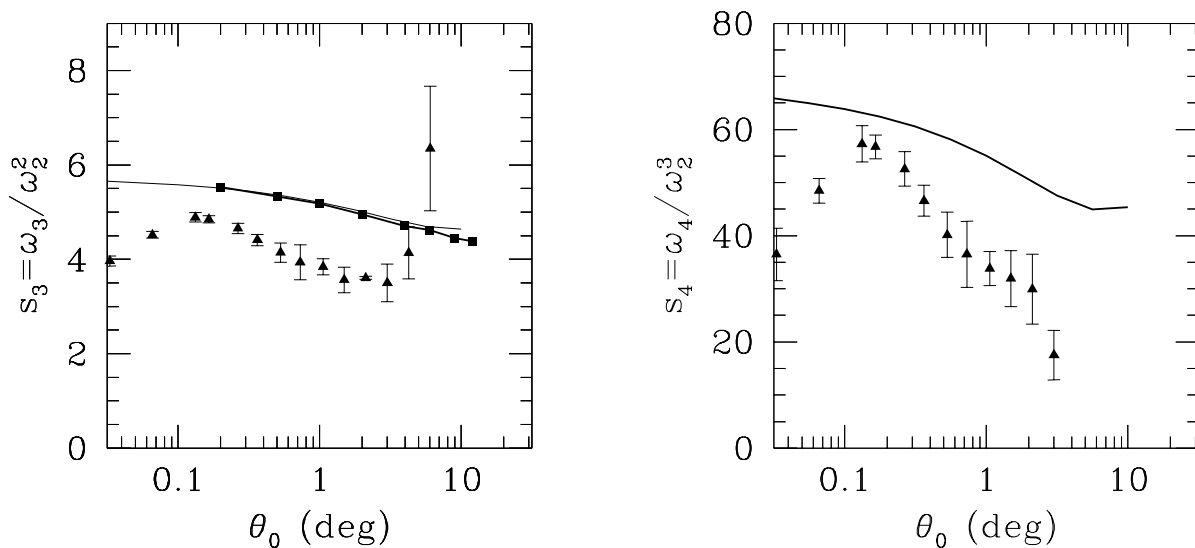


Figure 4. The $s_3(\theta)$ and $s_4(\theta)$ coefficients in the APM angular catalogue (triangles, see [19]) compared to the PT predictions, with the small angle approximation (solid lines), or with a numerical integration of the projection effects (squares).

There is still a significant discrepancy between the PT results and the observations. As the theoretical predictions are very robust with respect to uncertainties in the selection function or with respect to values of Ω and Λ (see [6]), it does not seem possible to reconcile the PT predictions with the observations, unless galaxies are biased. This bias is however less important than the one expected for the IRAS galaxies. These observations are anyway a strong indication in favor of Gaussian initial conditions. The implications of models with topological defects like string theories or textures have been investigated in particular by Gaztañaga [20]. He found that the current data, unless the galactic distribution is unrelated to the mass distribution(!), exclude such theories.

6 The Velocity Field Statistics

Although data on the peculiar velocities are more difficult to obtain, it is a very interesting domain of investigation since cosmic velocities are in principle directly related to the mass fluctuations. In a recent review, Dekel [15] has presented the observational and theoretical status of this rapidly evolving field.

The line-of-sight peculiar velocities are estimated from the Tully-Fisher (or similar) relation between the absolute luminosity of the galaxies and their internal velocity dispersion for elliptical, or their circular velocity for spirals. From these informations, and taking advantage of the expected absence of vorticity, it is possible to build the whole 3D smoothed velocity field. It has been done in particular

in [11, 17], using the so-called POTENT reconstruction method. A straightforward application of the reconstructed velocity field is the use of the velocity-density relationship obtained in the linear regime (6) that would indeed provide a way to measure Ω . This is possible however only if galaxies are not biased. Otherwise, assuming that at large scale, $\delta_{\text{galaxies}}^{(1)}(\mathbf{x}) = b \delta^{(1)}(\mathbf{x})$, the observations constrain a combination of Ω and b , $\beta = \Omega^{0.6}/b$. Various results for β have been given in the literature (see [15]). A rough compilation of them leads to $0.3 \lesssim \beta \lesssim 1.2$.

As we have no robust models for the large-scale bias of the galaxies, it is quite natural to explore the *intrinsic* properties of the velocity field. In the following, no assumptions are made on the bias, galaxies are simply assumed to act as *test particles* for the large-scale flows. Within this scheme Dekel & Rees [16] proposed to use the maximum expanding void to put constraints on Ω ; Nusser & Dekel [34] tried to reconstruct the initial density field using the Zel'dovich approximation, thus constraining Ω on the basis of Gaussian initial conditions. Here I present a more systematic study of the expected properties of the local divergence using PT.

In a similar way than for the density field it is indeed possible to compute the coefficients T_p that relate the high order moments of the local divergence to the second moment,

$$T_p = \langle \theta^p \rangle_c / \langle \theta^2 \rangle^{p-1}. \quad (22)$$

Unlike the S_p coefficients these ones are found to be strongly Ω dependent (but weakly Λ dependent),

$$T_p(\Omega) \propto \Omega^{-0.6(p-2)}, \quad (23)$$

as is a direct consequence of the time dependence of $\theta^{(i)}$ found in (7). The parameter $T_3(\Omega)$ was calculated in [8] as a function of Ω ,

$$T_3(\Omega) = \frac{1}{\Omega^{0.6}} \left[\frac{26}{7} + (n+3) \right], \quad (24)$$

and proposed as a possible indicator to measure Ω . A preliminary investigation using the POTENT data gave $\Omega > 0.3$ with a good confidence level.

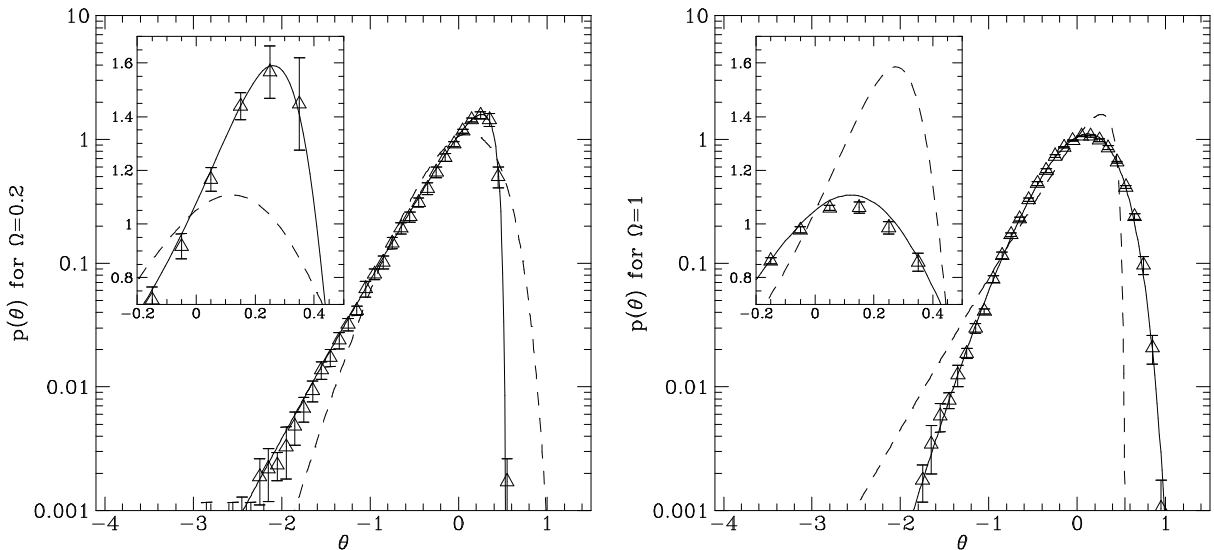


Figure 5. Comparison of the PT predictions for the shape of the PDF of the velocity divergence (solid lines) with results of numerical simulations for $n = -1$. In the left panel $\Omega = 0.2$ and in the right $\Omega = 1$. In both cases we have $\sigma_\theta \approx 0.4$. The dashed lines are the PT predictions when the reverse assumption is made on Ω .

But more generally the Ω dependence of the T_p coefficients obviously extends to the shape of the PDF of the local divergence. In particular we can show that for a power law spectrum with $n \approx -1$,

it is approximately given by,

$$\lambda = 1 - \frac{2\theta}{3\Omega^{0.6}}, \quad \kappa = 1 + \frac{\theta^2}{9\lambda\Omega^{1.2}}; \quad (25)$$

$$p(\theta) = \frac{\left([2\kappa - 1]/\kappa^{1/2} + [\lambda - 1]/\lambda^{1/2}\right)^{-3/2}}{\kappa^{3/4}(2\pi)^{1/2}\sigma} \exp\left[-\frac{\theta^2}{2\lambda\sigma^2}\right], \quad (26)$$

where σ is the rms of the fluctuations of θ . This distribution exhibits a strong Ω dependence as it can be seen on Fig. 5. As expected, when Ω is low the distribution is strongly non-Gaussian, with a sharp cut-off in the large divergence tails (it corresponds to rapidly expanding voids). This is this feature (discovered in an independent way) that was used in [16] to constrain Ω .

We have checked these theoretical predictions with numerical experiments (see Fig. 5) and found once again that the numerical results are in excellent agreement with them. It opens ways to have reliable measure of Ω from velocity data.

7 Conclusions

As this rapid overview have shown it, the study of the quasi-linear regime is in rapid development. A lot of efforts have been devoted to analytic calculations, and our understanding of the growth of structures in the intermediate regime has considerably improved. In particular comparisons with numerical simulations have shown that the PT results have a surprisingly large validity domain for the density as well as for the velocity fields. So far, most of the comparisons have been done for the cumulants at their leading order. However, the recent analytic results obtained for the next-to-leading order have open puzzling questions for their interpretation.

In any case, these PT results provide extremely discriminatory tools to test the gravitational instability scenarios. Comparisons with data have already provided valuable insights into the properties of the galaxy distribution: they have indeed given strong indications in favor of Gaussian initial conditions and have pointed out precious indications on the existence and nature of biases between the large-scale matter distribution and the galaxy distribution. Moreover, assuming Gaussian initial conditions, it seems possible to get reliable *and bias independent* constraints on Ω from the statistics of the large-scale cosmic flows.

Acknowledgements. I would like to thank Roman Scoccimarro and Enrique Gaztañaga for permission to include some of their figures.

References

- [1] Balian, R. & Schaeffer, R. 1989, *Astr. & Astrophys.* **220**, 1
- [2] Baugh, C.M., Gaztañaga, E. & Efstathiou, G., 1994, *Mon. Not. R. astr. Soc.* in press
- [3] Bernardeau, F. 1992, *Astrophys. J.* **292**, 1
- [4] Bernardeau, F. 1994, *Astrophys. J.* **433**, 1
- [5] Bernardeau, F. 1994, *Astr. & Astrophys.* **291**, 697
- [6] Bernardeau, F. 1995, *Astr. & Astrophys.* **301**, 309
- [7] Bernardeau, F. & Kofman, L., 1995, *Astrophys. J.* **443**, 479
- [8] Bernardeau, F., Juszkiewicz, R., Dekel, A. & Bouchet, F. 1995, *Mon. Not. R. astr. Soc.* **274**, 20
- [9] Bernardeau, F. & Van de Weygaert, R. 1996, *Mon. Not. R. astr. Soc.* **279**, 693
- [10] Bernardeau, F., Van de Weygaert, R., Hivon, E. & Bouchet, F. in preparation
- [11] Bertschinger, E., Dekel, A., Faber, S.M., Dressler, A. & Burstein, D. 1990, *Astrophys. J.* **364**, 370

- [12] Bouchet, F., Juszkiewicz, R., Colombi, S. & Pellat, R., 1992, *Astrophys. J.* **394**, L5
- [13] Bouchet, F., Strauss, M.A., Davis, M., Fisher, K.B., Yahil, A. & Huchra, J.P. 1993, *Astrophys. J.* **417**, 36
- [14] Colombi, S., Bouchet, F.R. & Schaeffer, R. 1995, *Astrophys. J. Suppl. Ser.* **96**, 401
- [15] Dekel, A. 1994, *Annual Review of Astr. & Astrophys.* **32**, 371
- [16] Dekel, A. & Rees, M.J. 1994 *Astrophys. J.* **422**, L1
- [17] Dekel, A., Bertschinger E. & Faber, S.M. 1990, *Astrophys. J.* **364**, 349
- [18] Fry, J., 1984, *Astrophys. J.* **279**, 499
- [19] Gaztañaga, E., 1994, *Mon. Not. R. astr. Soc.* **268**, 913
- [20] Gaztañaga, E., preprint, astro-ph/9512008
- [21] Gaztañaga, E. & Frieman J. 1994, *Astrophys. J.* **437**, L13
- [22] Goroff, M.H., Grinstein, B., Rey, S.-J. & Wise, M.B. 1986, *Astrophys. J.* **311**, 6
- [23] Hamilton, A.J.S., Kumar, P., Lu, E. & Matthews, A. 1991 *Astrophys. J.* **374**, L1
- [24] Hivon, E., Bouchet, F., Colombi, S., Juszkiewicz, R. 1995, *Astr. & Astrophys.* **298**, 643
- [25] Jain, B. & Bertschinger, E. preprint, astro-ph/9503025
- [26] Juszkiewicz, R. 1981, *Mon. Not. R. astr. Soc.* **197**, 931
- [27] Juszkiewicz, R., Bouchet, F.R. & Colombi, S. 1993, *Astrophys. J.* **412**, L9
- [28] Juszkiewicz, R., Weinberg, D. H., Amsterdamski, P., Chodorowski, M. & Bouchet, F., 1995, *Astrophys. J.* **442**, 39
- [29] Lahav, O. Itoh, M. Inagaki, S. & Suto, Y. 1994 *Astrophys. J.* **402**, 387
- [30] Lahav, O., Lilje, P.B., Primack, J.R. & Rees, M. 1991 *Mon. Not. R. astr. Soc.* **251**, 128
- [31] Lokas, E., Juszkiewicz, R., Weinberg, D.H., Bouchet, F.R., preprint, astro-ph/9407095
- [32] Lokas, E., Juszkiewicz, R., Hivon, E., Bouchet, F.R., preprint, astro-ph/9508032
- [33] Makino, N, Sasaki, M., Suto, Y. 1992 *Phys. Rev. D* **46**, 585
- [34] Nusser, A., Dekel, A. 1993 *Astrophys. J.* **387**, 405437
- [35] Peebles, P.J.E. 1980; *The Large-Scale Structure of the Universe*; Princeton University Press, Princeton, N.J., USA;
- [36] Pollo, A. & Juszkiewicz, R. in preparation
- [37] Scoccimarro, R. & Frieman, J., preprint, astro-ph/9509047
- [38] Scoccimarro, R. & Frieman, J., preprint, astro-ph/9602085

Résumé

La compréhension de la formation des grandes structures requiert la résolution d'équations non-linéaires couplées décrivant l'évolution des champs de densité et de vitesse cosmologiques. C'est un problème compliqué qui, ces dix dernières années, a été traité essentiellement avec des simulations numériques à N corps. Il y a cependant un régime, le régime dit quasi-linéaire, pour lequel les fluctuations relatives de densité sont inférieures à l'unité en moyenne. Il est alors possible d'utiliser des techniques de théorie des perturbations où les développements perturbatifs sont faits par rapport aux fluctuations initiales. Je présente ici les résultats majeurs qui ont été obtenus dans ce régime.